NeuroImage: Clinical 12 (2016) 198–211

Contents lists available at ScienceDirect

NeuroImage: Clinical

journal homepage: www.elsevier.com/locate/ynicl

Bedside functional brain imaging in critically-ill children using high-density EEG source modeling and multi-modal sensory stimulation

Danny Eytan[a], Elizabeth W. Pang[b], Sam M. Doesburg[c], Vera Nenadovic[b], Bojan Gavrilovic[d], Peter Laussen[e], Anne-Marie Guerguerian[f,*,1,2]

[a]Department of Critical Care Medicine, Neurosciences and Mental Health Program, Research Institute, The Hospital for Sick Children, University of Toronto, Toronto, Canada
[b]Division of Neurology, Department of Paediatrics, Neurosciences and Mental Health Program, Research Institute, The Hospital for Sick Children, University of Toronto, Toronto, Canada
[c]Department of Biomedical Physiology and Kinesiology, Behavioural and Cognitive Neuroscience Institute, Simon Fraser University, Burnaby, Canada
[d]Institute of Biomaterials and Biomedical Engineering, Department of Critical Care Medicine, Neurosciences and Mental Health Program, Research Institute, The Hospital for Sick Children, University of Toronto, Toronto, Canada
[e]Department of Critical Care, David and Stacey Cynamon Chair in Critical Care Medicine, The Hospital for Sick Children, Department of Anaesthesia, University of Toronto, Toronto, Canada
[f]Department of Critical Care, Neuroscience and Mental Health Program, Research Institute, The Hospital for Sick Children, University of Toronto, Toronto, Canada

ARTICLE INFO

Article history:
Received 27 July 2015
Received in revised form 24 June 2016
Accepted 30 June 2016
Available online 04 July 2016

Keywords:
Bedside cerebral function
Children
Brain injury
Electroencephalography (EEG)
Evoked potentials
Neuroimaging
Pediatrics

ABSTRACT

Acute brain injury is a common cause of death and critical illness in children and young adults. Fundamental management focuses on early characterization of the extent of injury and optimizing recovery by preventing secondary damage during the days following the primary injury. Currently, bedside technology for measuring neurological function is mainly limited to using electroencephalography (EEG) for detection of seizures and encephalopathic features, and evoked potentials. We present a proof of concept study in patients with acute brain injury in the intensive care setting, featuring a bedside functional imaging set-up designed to map cortical brain activation patterns by combining high density EEG recordings, multi-modal sensory stimulation (auditory, visual, and somatosensory), and EEG source modeling. Use of source-modeling allows for examination of spatio-temporal activation patterns at the cortical region level as opposed to the traditional scalp potential maps. The application of this system in both healthy and brain-injured participants is demonstrated with modality-specific source-reconstructed cortical activation patterns. By combining stimulation obtained with different modalities, most of the cortical surface can be monitored for changes in functional activation without having to physically transport the subject to an imaging suite. The results in patients in an intensive care setting with anatomically well-defined brain lesions suggest a topographic association between their injuries and activation patterns. Moreover, we report the reproducible application of a protocol examining a higher-level cortical processing with an auditory oddball paradigm involving presentation of the patient's own name. This study reports the first successful application of a bedside functional brain mapping tool in the intensive care setting. This application has the potential to provide clinicians with an additional dimension of information to manage critically-ill children and adults, and potentially patients not suited for magnetic resonance imaging technologies.

1. Introduction

Acute brain injury is a common cause for hospitalization in pediatric and adult intensive care units with traumatic brain injury being the leading cause of death in children and young adults (Moreau et al. 2013; Parslow et al. 2005). Common other causes of acquired brain injury are strokes, intracranial hemorrhages, meningoencephalitis, tumors and hypoxic ischemic encephalopathy associated with cardiopulmonary arrest. All are associated with significant personal, social and economic burdens (Geocadin et al. 2008; Corso et al. 2006; Perkins et al. 2009). As these patients are often critically-ill and sometimes have associated metal hardware attached or implanted, routine brain imaging with modalities such as MRI or Computed Tomography (CT) are not feasible. Even when MRI is performed, it is usually in the later stages of the illness and is infrequently acquired. CT also has associated radiation exposure and a lower resolution. Critically, both clinical MRI and CT can detect anatomical but not functional alterations following brain injury and modalities such as PET and fMRI are not broadly available at such stages of the illness. A system that can be applied at the bedside

* Corresponding author.
E-mail address: anne-marie.guerguerian@sickkids.ca (A.-M. Guerguerian).
[1] Laboratory address: Peter Gilgan Centre for Research and Learning, 686 Bay Street, 8th Floor South, 08.9709, Toronto, Ontario, Canada, M5G 0 A4.
[2] Administrative and mailing address: The Hospital for Sick Children, Department of Critical Care, Second Floor Atrium, Room 2830-A, 555 University Avenue, Toronto, Ontario, Canada, M5X 1G8.

http://dx.doi.org/10.1016/j.nicl.2016.06.021

of critically-ill patients and provide functional mapping and continued neuromonitoring, may offer opportunities for earlier detection of neurological injury, aid in guiding therapy and improve outcomes (Vidgeon and Strong 2011).

Electroencephalography (EEG) is a noninvasive modality with bedside availability that measures voltage fluctuations resulting from ionic current flows within the neurons of the brain, mostly as a result of synchronized synaptic activation to pyramidal cortical neurons (Niedermeyer and da Silva 2005). EEG waveforms recorded at the scalp reflect cortical activity through the summation of excitatory postsynaptic action potentials arising mainly from the pyramidal neurons in cortical layers III, V and VI with contribution from glial cells (Buzsáki et al. 2003; Ebersole 2003). There are associations between the EEG signal and other functional recording modalities such as fMRI and magnetoencephalography (MEG) (Singh et al. 2003). EEG use in intensive care settings in the context of acute brain injury is often limited to the detection of subclinical seizures and of encephalopathic features. Some studies have shown the utility of EEG signals to assist in the prediction of outcomes and to follow recovery after traumatic brain injuries (Duncan et al. 2011; Nenadovic et al. 2008; Ramachandran Nair et al. 2005), and in hypoxic ischemic encephalopathy (Wijdicks et al. 2006; Nishisaki et al. 2007).

Evoked Potentials (EPs) are electrical signals triggered by various sensory or cognitive stimuli that reflect the time course of information processing in the brain, thereby allowing for assessment of somatosensory, auditory, visual, cognitive and emotional processing pathways in healthy and brain-injured patients (Lehembre et al. 2012; Picton et al. 2000; Fernandez-Espejo and Owen 2013; Fischer et al. 2008; Daltrozzo et al. 2007). There are some reports on the use of EPs in the context of severe head injuries (Robinson et al. 2003; Folmer et al. 2011; Lew et al. 2006; Kane et al. 1996) mainly the somatosensory evoked potential (SEP) with only a few studies reporting the use of continuous SEP in the context of traumatic brain injury (Amantini et al. 2009).

In the present study, we implemented a bedside functional neuromonitoring system that combined high-density EEG monitoring with multi-modal sensory stimulation and EP recordings. The electrical signals captured with such a system allows for the generation of functional brain images by source modeling, as is commonly done in cognitive neuroscience (Lee et al. 2014), as has been reviewed previously (Murray et al. 2004). Use of EEG and EPs are becoming more prevalent in studies of patients with decreased levels of consciousness (Harrison and Connolly 2013). Some researchers have also suggested that in traumatic brain injuries it may be useful to combine these electrophysiological measures with imaging modalities such as CT and MRI (Duncan et al. 2011; Irimia et al. 2013a; Irimia et al. 2013b).

Such a bedside system as described in this proof of concept study may prove valuable for early diagnosis and detection of cerebral dysfunction in order to guide therapy in injured patients and to facilitate understanding of the functional brain state in subjects with a decreased level of responsiveness. Having a portable system that can be deployed at bedside presents many advantages over MEG and fMRI which require moving patients into the scanner and restricts recording durations (e.g., over several days and nights).

2. Materials and methods

2.1. Participants

Ten healthy volunteers (six males and four females) and five critically-ill patients (three males and two females) participated in this study. The healthy volunteers ranged in age from 7 to 16 years (median 12 years) and nine were right-handed. The patients were aged from 2.5 to16 years (median 8.5 years); all with acute brain injury of various etiologies (traumatic brain injury, hemorrhagic stroke, necrotizing encephalitis or ischemic stroke). In these patients, all recordings were done in the critical care unit while subjects were in the acute phase of their illness (less than one week of admission to hospital). All participants' guardians provided informed written consent and when applicable participants provided assent. This study was approved by Research Ethics Board of The Hospital for Sick Children's in Toronto, Ontario, Canada.

2.2. Experimental set-up, procedure and recording

The set-up consisted of a high-density EEG coupled with three multi-modal sensory stimulation generators: visual, auditory and somatosensory. This set-up was mounted on a small mobile cart to enable bedside recordings within the critical care unit (for either private or multiple patient rooms). The set-up was tested and approved by the Biomedical Engineering Department of The Hospital for Sick Children.

2.2.1. EEG recordings

The QuikCap electrode cap (Compumedics Neuroscan, El Paso, TX) was used for EEG electrode placement. The stretchable electrode cap contained 64 Ag–AgCl electrodes arranged according to the modified 10–20 system of electrode placement (Guideline 5 2006). The advantages of electrode caps are two-fold: they can be applied quickly and easily, which is essential in the critical care unit, and electrode positions can be reliably calculated by referencing common anatomical landmarks. The reference electrode was positioned near the vertex between the Cz and CPz electrodes and the ground electrode was located over the frontal area of the scalp, between the Fz and FPz electrodes. Electrode impedances were <10 kΩ.

An average reference montage was used for visualization and analysis (Cuffin 2001; Michel et al. 2004). Continuous EEG data from 64 channels were recorded throughout each stimulation session using a Neuroscan RT system (Compumedics Neuroscan, El Paso, TX) with exact time stamping of the sensory stimuli. Data were digitized at 1000 Hz and low-pass filtered at DC-200 Hz for visual and auditory stimulation and digitized at 5000 Hz and low-pass filtered at DC-1000 Hz for somatosensory stimulation.

2.2.2. Sensory stimulation

Multi-modal sensory stimuli were provided using standard equipment and driven by a laptop running custom-made software using Matlab (The Mathworks, Natick, MA, USA) and the Psychophysics Toolbox (Brainard 1997) according to standard clinical guidelines (International Federation of Clinical Neurophysiology)). The stimulation computer and software was used to control the sensory modality, stimulus parameters (timing, duration, amplitude, pitch etc.) and was paired with an EEG recording computer via a serial port, to allow exact time stamping of stimuli delivery, and to the stimulation equipment using an Arduino UNO controller. Each recording session lasted approximately 1 h and included both multi-modal stimulation and baseline resting state EEG recordings.

Visual stimuli were presented using a standard xenon flash lamp (XLTek XLPS-1 Photic stimulator, Stellate, Montreal, Canada) and consisted of 300 stroboscopic light flashes (23 W/m^2) at a rate of 2 Hz.

Somatosensory stimulation was presented via median nerve stimulation using a Grass S12 biphasic stimulator (Grass instruments, Quincy, MA, USA). Stimuli consisted of 300 stimuli (square wave, 200 μsec duration) for each arm at a rate of 2 Hz. Stimuli were delivered to the median nerve at the wrist, at an intensity just above each individual's motor threshold.

Auditory stimuli were delivered using headphones at an intensity of 80 dB using two different oddball paradigms. A tone-based paradigm consisted of “rare”-deviant (probability of 0.2, 1100 Hz, duration 75 msec, rise and fall times of 5 msec) and “common”-standard (probability 0.8, 1000 Hz, duration 75 msec, rise and fall times of 5 msec) tones to induce a mismatch negativity (see citations (36–38)). Deviant stimuli were interspersed randomly between the standard tones.

However, the stimulation sequence was generated so that it did not contain two consecutive deviant stimuli. A total of 1250 tone stimuli (1000 standard and 250 deviant tones) were delivered in each recording session at a rate of 2 Hz. For all participants, <0.5% of the stimuli were discarded due to technical issues related to time stamping failure. Participants were asked to report any prior hearing abnormalities but no formal hearing test was done before enrollment. The physical examination or neuroimaging (e.g., mastoids) did not reveal auditory canal anomalies in critically-ill subjects.

In light of recent reports on heterogeneous alterations in cortical processing in comatose patients (Fernandez-Espejo and Owen 2013; Daltrozzo et al. 2007; Staffen et al. 2006), we also presented voice auditory stimuli using two oddball names paradigms: one in which the deviant stimulus had no emotional meaning (a common name) and one in which the deviant stimulus was the subject's own name (SON) (Berlad and Pratt 1995). The names were recorded in the English language by each participant's parent and the difference between the deviant and standard name in each oddball pair was the first vowel only, thus preserving stimulus length and general envelope. A total of 1800 name stimuli trials (900 for each name-pair, deviant probability of 0.2) were delivered in each recording session at a rate of 1 Hz. Using a dual paradigm allowed us to examine the cortical effects of processing a deviant stimulus with higher-level complexity compared to a tone but also to study the additive effect of the emotional content of the deviant word. In order to comply with local regulatory oversight, we verified that each medical device used to record signals was Health Canada approved for use in humans at the time of the study. In order to ensure additional safety of critically-ill children, the entire experimental set-up on a mobile cart was tested and approved for use in the intensive care setting by the institutional Biomedical Engineering service. As the recording session lasted approximately an hour for each participant with ~4000 stimuli and in order to avoid fatigue we refrained from repetitions of the entire paradigm. As the number of stimulus presentations for each modality was in the hundreds we indirectly verified reproducibility by comparing the average evoked responses to the first and last 100 stimuli for each participant and sensory modality. For example, for visual flash stimuli whose responses are known to be variable and for electrodes FPz, O1, O2, Oz (traces are shown in Fig. 1A) the average correlation coefficient between the evoked potential traces to the first and last 100 stimuli for all healthy participants was 0.77 ± 0.19.

2.3. Data analyses

2.3.1. Preprocessing and artifact rejection

Continuous EEG recordings were segmented into epochs of either 600 msec peri-stimuli (−100 msec to 500 msec post-stimulus time) for the somatosensory, auditory and visual stimuli or 1100 msec (−100 msec to 1000 msec post-stimulus time) for the name conditions. Stimulation artifacts for somatosensory evoked potentials were removed from −4 to +4 msec peri-stimulation. Data were de-trended and the baseline was corrected (−100 msec to stimulus onset) automatically for all epochs and then averaged for each subject according to stimulus identity, yielding nine different evoked potential types: one visual, two somatosensory (right, left arm), and six auditory (standard tone, deviant tone, two different standard names, deviant name and the subject's own name). Noisy electrodes were rejected for each subject according to visual inspection of the data. For each healthy participant an average of 60 ± 2.5 electrodes were included for analysis and 57 ± 2.5 electrodes were included for brain-injured critically-ill children, reflecting the associated technical challenges.

In order to avoid a selection bias, we refrained from automatic trial rejection by voltage criteria as sedated patients and those with severe brain injury frequently have EEG patterns with high voltage slow waves, which should be captured due to possible relevance for brain function (Schiff et al. 2014; Hirsch 2004). To prevent bias in our results, we conducted a preliminary analysis with the above criteria which resulted in a rejection rate of <10% for the healthy participants and no qualitative changes in the results due to the large number of repetitions for each stimulus type (data not shown).

Data presented in this study were not filtered prior to analyses and source reconstruction except for short latency (<35 msec post-stimulus) somatosensory evoked potentials for which the average EPs were band-pass filtered at 30–300 Hz to allow examination of the high-frequency component of the evoked response at the source level. Traces in Figs. 1 and 4 were filtered at 0.5–40 Hz for visualization purposes only.

2.3.2. Defining time periods of interest

Examination of the averaged Global Field Power (GFP, spatial root mean squared across all electrodes) for each stimulus type was used to define time periods of interest as detailed in (Michel et al. 2004). Time periods of interest were then used to study the cortical activation traces at the source level by integrating the cortical activation over each time period. The two major approaches aimed at defining the time periods of interest for source localization are the “component approach” relying on standard traditionally expected peaks (such as the N100 and P300) and using the peaks of the Global Field Power (GFP) as a guide to locate stable phases of cortical activation. The GFP has the advantage of being a global measurement of the electric field at the scalp, which is aided by the increased number of electrodes and is not biased by the experimenter's selection of a limited number or distribution of electrodes.

2.3.3. Brain source modeling

EEG source imaging entails using the scalp's electrical data to estimate the locations of active sources in the brain, and has been recently reviewed by Michel and colleagues (Michel et al. 2004). Source imaging of high-density EEG data (43) is increasingly used as a brain imaging method for research purposes (Michel and Murray 2012) and has also been incorporated into clinical practice (Brodbeck et al. 2011). The cortical generators of the average EPs were estimated for each participant and stimulus type using the Brainstorm toolbox (Tadel et al. 2011). This toolbox was also used for analysis and visualization of the source reconstructed brain activation maps. The conductive head volume was modeled according to a 3-sphere method (Berg and Scherg 1994). A standard set of electrode positions was used for the construction of the forward model. For all participants, for the head model calculation, source imaging and projection, we used the default anatomy in Brainstorm which is based on the Colin27 MRI volume provided by the Montreal Neurological Institute (MNI) (Holmes et al. 1998) as an MRI was not available for our healthy participants. While using this template may have some limitations in children, and some pediatric MRI templates are now available, we opted for the default template which would allow others to consider using our approach more readily in healthy participants. For all brain-injured patients, as they underwent MRI, we also extracted the segmented brain surfaces from their T1-weighted MRI images using Freesurfer image analysis suite (http://surfer.nmr.mgh.harvard.edu/) or Brainsuite (Shattuck and Leahy 2002) and used them to recalculate the head model and the source imaging. These were then used to compare the source activation results to the ones generated by using a canonical head model. Comparison of the source activation using the standard canonical MRI to that generated by using the individual participant MRI, when available, did not show qualitative differences, as can be seen in Fig. 6 and as examined quantitatively in Fig. 7.

The source solution space was constrained to the cerebral cortex, which was modeled as a three-dimensional grid of 15,002 vertices. There are many different source localization methods described in the literature. Of the instantaneous, 3D, discrete, linear solutions for the EEG inverse problem LORETA (Pascual-Marqui et al. 1994) is commonly used: a laplacian-weighted variant of the minimum norm estimation. Specifically in this study the inverse problem was solved by applying

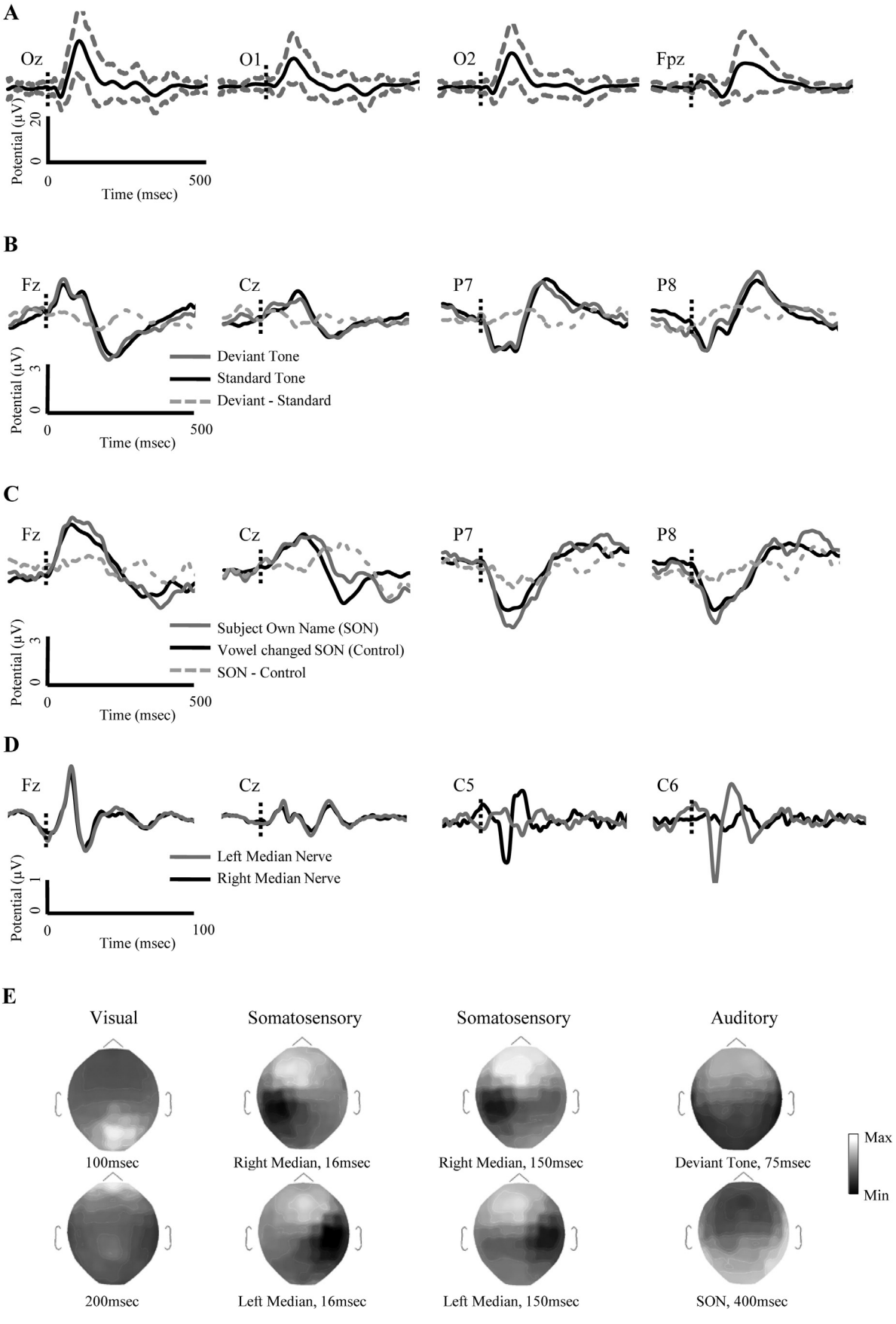
A
Oz
O1
O2
Fpz
Potential (μV)
20
0
0
500
Time (msec)
B
Fz
Cz
P7
P8
Deviant Tone
Standard Tone
Deviant - Standard
Potential (μV)
3
0
0
500
Time (msec)
C
Fz
Cz
P7
P8
Subject Own Name (SON)
Vowel changed SON (Control)
SON - Control
Potential (μV)
3
0
0
500
Time (msec)
D
Fz
Cz
C5
C6
Left Median Nerve
Right Median Nerve
Potential (μV)
1
0
0
100
Time (msec)
E
Visual
Somatosensory
Somatosensory
Auditory
100msec
Right Median, 16msec
Right Median, 150msec
Deviant Tone, 75msec
Max
Min
200msec
Left Median, 16msec
Left Median, 150msec
SON, 400msec

an unconstrained sLORETA (Pascual-Marqui 2002) method implemented as a routine of the Brainstorm platform, which allows a noise-normalized estimation of the distribution of electrical sources in the brain. The noise covariance matrix was estimated for each participant from the 100 msec epochs prior to stimuli presentation. As noted above, for each participant, the sources were projected to the standard anatomical template (MNI) (Evans et al. 1993), as well as their individual MRI when available for the patient group only. Of note, using different methods for source estimation (Weighted Minimum Norm, constrained LORETA and others) did not qualitatively change the main results presented here (data not shown).

2.3.4. Defining cortical regions of interest

In order to investigate the time course of functional responses originating from specific brain systems, to support the development of an automated monitoring tool and to provide summary information regarding the functional responses of a manageable set of functional brain systems, the cortical surface was divided into 12 functional Cortical Regions of Interest (Cortical-ROIs) which spanned the entire cortex. This was done using the Desikan-Kiliany atlas (Desikan et al. 2006), a gyrus-based region of interest in the cortical atlas, and by grouping regions according to their dominant function according to published scientific literature. Thus, from 68 different ROIs in the original atlas, we derived 12 cortical-ROIs (six for each hemisphere) reflecting Somatosensory/Motor, Language, Memory/Emotion, Auditory, Visual and Executive Control systems (see Fig. 4). Time courses of cortical-ROI activation were derived by using the scout analysis tool in Brainstorm and by averaging the source activation over the subsets of neighboring vertices in each region, similar to what was done by (Mento et al. 2013). These activation traces were also averaged over time according to the time periods of interest as described above. When performing statistical tests on the time and region averaged activation traces, a Bonferroni correction for multiple comparisons was used and a MANOVA test was applied when applicable.

In this report, all the data recorded were used for analysis except in one patient (Subject 1) due to technical difficulties associated with a poor fitting of the head cap and a technical error in EEG filtering. For this recording, visual and somatosensory recordings had to be discarded but auditory data are reported.

3. Results

3.1. System validation at the sensor level

The potential to generate reliable multi-modal cortical EPs, using this set-up and experimental protocol, was initially tested on 10 healthy volunteers with group-averaged traces presented in Fig. 1. Fig. 1A shows sample group-averaged traces for four electrodes following light flashes. A large occipital response (~10-15 μV; 100 msec) is followed by a smaller late (160 msec) and more variable frontal activation. This frontal activation was seen in half of the healthy controls and has been reported elsewhere as well (Di Russo et al. 2002). Panels B and C in Fig. 1 depict the average evoked response to auditory stimulation and the Mismatch Negativity (MMN) effect, ranging between 0.2 μV ± 0.2 μV to 0.5 μV ± 0.09 μV for tone and word stimuli respectively. A specific contralateral central cortical EP trace following somatosensory stimulation was evident at short latencies (as can be seen in panel D) but was also observed at much longer latencies (as seen at 150 msec in the scalp potential map in Fig. 1E) up to 350 msec. The post-stimulus times for these topographical maps were chosen according to the GFP peaks as detailed in the methods section. These maps demonstrate statistically significant activity compared to baseline (−100 to 0 msec prior to stimulus presentation) with an average corrected p-values < 0.00001 for each topographical map (parametric t-test with false discovery rate correction).

3.2. System validation at the source level in healthy children

As reviewed in (Michel et al. 2004), while scalp potential maps are the precursor for source localization, they provide limited information about the location and distribution of the cortical sources. Source modeling methods are more informative regarding the locations of generators. Fig. 2 depicts the group-averaged cortical activation as measured in the healthy participants for three sensory modalities. Source reconstruction for this figure and throughout this report was done using sLORETA, a well-established, noise-normalized source modeling method (Pascual-Marqui et al. 1994). For each modality, we identified 3–4 time periods of interest (time-ROIs) over which the cortical activation was averaged. These time periods were chosen according to the Global Field Power (GFP) trace of the EP responses for each modality. Visual flash stimuli generated a reliable occipital response beginning at ~50 msec, peaking at 100–125 msec with additional frontal activation occurring slightly later. In contrast, somatosensory stimulation of the median nerve was followed by a rapid cortical response starting at ~14 msec post-stimulus and localized to the contralateral somatosensory areas. This initial high-frequency response was followed by a slow wave of activation lasting up to 350 msec and localized to the same cortical areas. As noted above, auditory tone stimuli were delivered in an oddball paradigm. While a marked bilateral response in the auditory cortices was seen for the standard and deviant stimuli (Figs. 2 and 4B), the late (225–275) response was significantly larger for the deviant stimuli compared to the standard tone (average amplitude of 552pA.m versus 374pA.m, $p < 0.01$, paired t-test). In summary, it can be seen from Fig. 2 that by combining stimuli from different modalities the evoked cortical responses span most of the cortical surface, yet responses are concentrated in brain areas known to correspond to the stimulation modality.

In order to investigate higher-level processing, we used two additional oddball paradigms involving words – one in which the deviant stimulus was the participant's own name (SON) and the other in which the deviant was an emotionally-neutral name. The difference in both paradigms between the deviant and the standard word was a single vowel change. Such a paradigm enabled us to test both paradigms for auditory stimuli processing of higher complexity than simple tones by comparing each deviant-standard pair and testing for preferential activation to stimuli with an emotional content by comparing the responses of the two deviants. Fig. 3 depicts the group-average activation to the oddball paradigm in which the deviant is the subject's own name. Similar to tone stimuli, we observed an initial bilateral response involving the auditory and temporal areas with late prominent right auditory activation which was significantly larger for the subject's own name ($p < 0.01$, paired t-test, testing over the auditory cortices) than to the standard word. A stronger activation was also seen in these areas to the other word deviant but these did not reach statistical significance. Moreover, when comparing the relative activation between the two deviants at the cortical-ROI level there did not seem to be a statistically significant larger effect to the subject's own name compared to the other deviant word at the group level.

Fig. 1. Group-average evoked responses: Panels A–D show evoked responses for representative recording electrodes averaged across healthy participants. A — Evoked responses for visual flash stimuli (300 stimuli per subject). Dashed grey lines mark ± standard deviation. B — Evoked responses for auditory tone stimuli (1000 standard (1000 Hz) and 250 deviant (1100 Hz) stimuli per subject). Also shown is the difference with a grey, dashed line. C — Evoked responses for auditory word, Subject's Own Name (SON) stimuli (720 standard (vowel-changed SON) and 180 deviant (SON) stimuli per subject). The differences are depicted by the grey dashed lines. Data for all of the above were filtered 0.5–40 Hz for visualization. D — Evoked responses to somatosensory stimulation of the right and left median nerves (300 stimuli per subject for each nerve; data filtered at 30–300 Hz). E — Scalp potential maps at different post-stimulus times and sensory modalities.

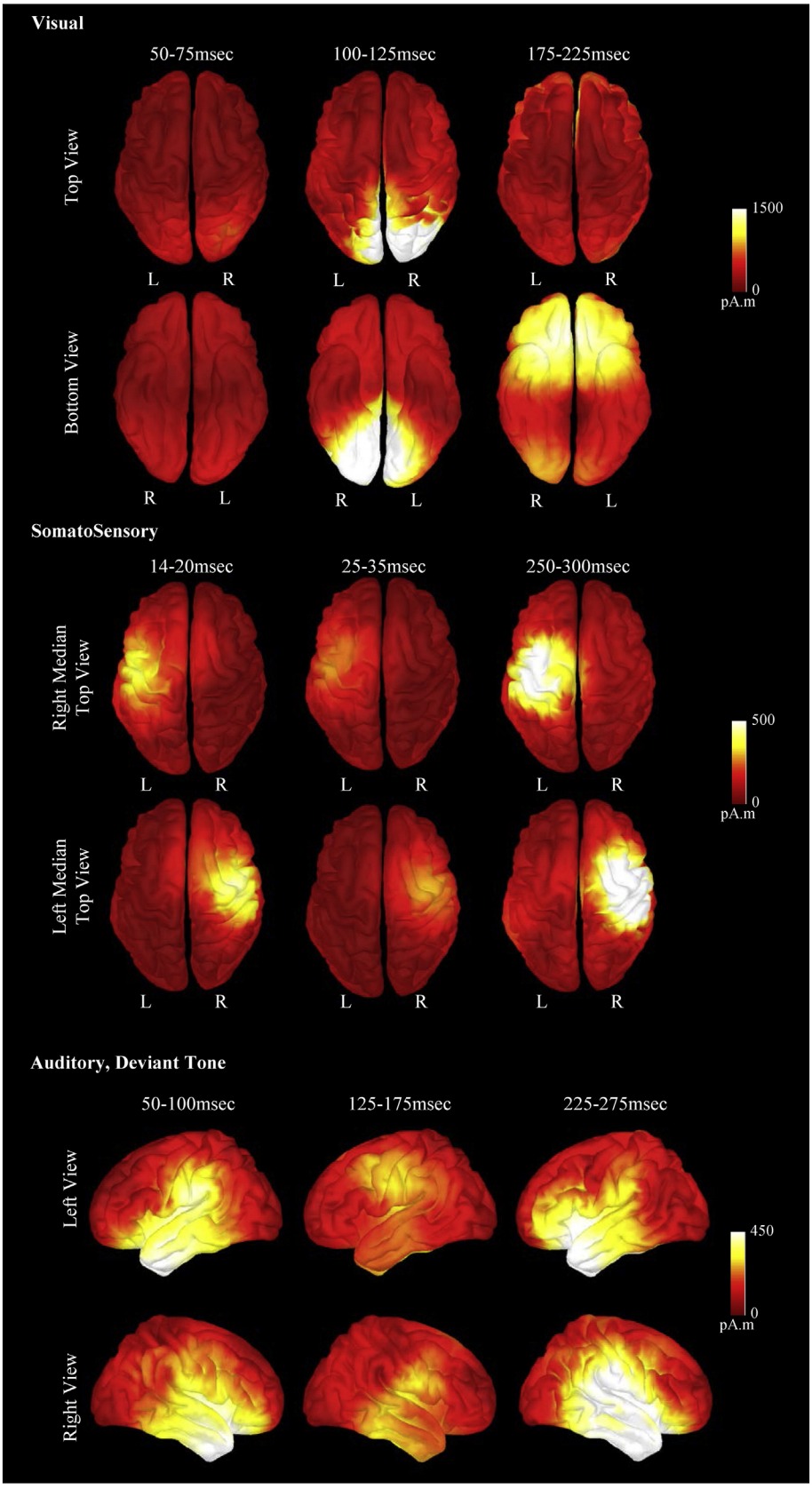

Fig. 2. Average evoked cortical activation: Group-averaged (healthy participants) cortical activations for specific sensory modalities and time-ROI.
Source activations derived using unconstrained sLORETA, normalized to individual noise covariance matrices and projected on a default generic MRI. Source activation for somatosensory stimulation for time-ROIs of 14–20 msec and 25–35 msec derived from band-pass filtered EPs of each subject at 30–300 Hz to enable evaluation of the high-frequency component of the early response.

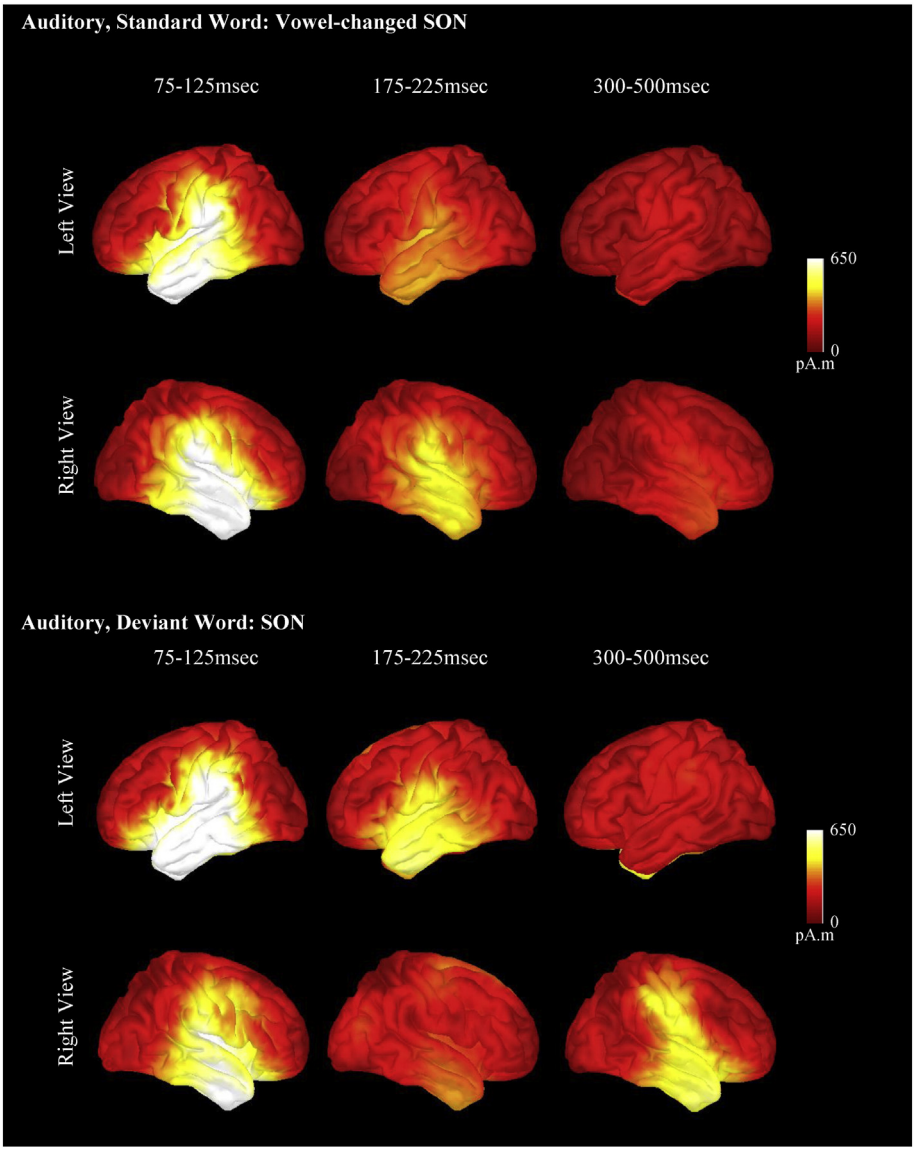

Fig. 3. Average evoked cortical activation to auditory word stimuli: Group (healthy participants) averaged cortical activations for auditory oddball stimulation with the deviant as the subject's own name (SON) and the standard stimuli as the same name with the first vowel changed, for three time-ROIs.
Source activations derived using unconstrained sLORETA, normalized to individual noise matrices and projected on a default generic MRI.

Using source modeling, together with a cortical-ROI approach, we transformed sensor-level EP traces into a relatively small number of source level time series reflecting activity within functional subsystems of the brain, obtained by averaging across voxels in the sLORETA source solution. This is ideal for continued neuromonitoring as it provides a traceable number of indices reflecting the function of various systems. Fig. 4A depicts the functional cortical-ROI parcellation we used – a total of 12 cortical functional areas were derived from the 68 ROI in the Desikan-Killiany atlas (Desikan et al. 2006). Fig. 4B shows the group average activation over time for each cortical-ROI in response to different sensory stimuli.

3.3. Towards a real-time monitor – generation of activation norms

The requirements for a successful system are that it be accurate, precise, sensitive and specific. As this was a first proof-of-principle study on a relatively small sample, an exhaustive validation is not possible but an appraisal for the potential to serve as a functional mapping and monitoring system can be derived. Fig. 5A demonstrates repeated cortical source activation estimates for one healthy subject. Each row represents five estimates, each derived from the EP trace averaged over 60 consecutive stimulus presentations (for a total of 300 per stimulus modality for the entire row). The source activation traces were averaged over a time-ROI of either 15–35 msec for the somatosensory stimulation or 50–150 msec for the visual evoked potentials. Thus, any given image of the 15 in Fig. 5A represents the source activation estimate as averaged for responses recorded over 30 s of stimulation.

Next, we attempted to define how specific each stimulation modality was in terms of selectively activating the corresponding brain system. This analysis was performed for our entire population of participants, both healthy and brain-injured. For each sensory modality, we calculated the fold average activation in its corresponding cortical-ROI relative to another control cortical-ROI. Specifically, we compared visual versus ipsilateral somatosensory (time-ROI 75–125 msec), auditory versus ipsilateral somatosensory (time-ROI 75–125 msec) and somatosensory versus contralateral somatosensory (time-ROI 15–35 msec). For example, to calculate the fold average activation for the left visual cortical-ROI we divided left visual activation 75–125 msec by left somatosensory activation 75–125 msec following visual stimulation. Fig. 5B depicts the logarithm of these values as averaged over 300

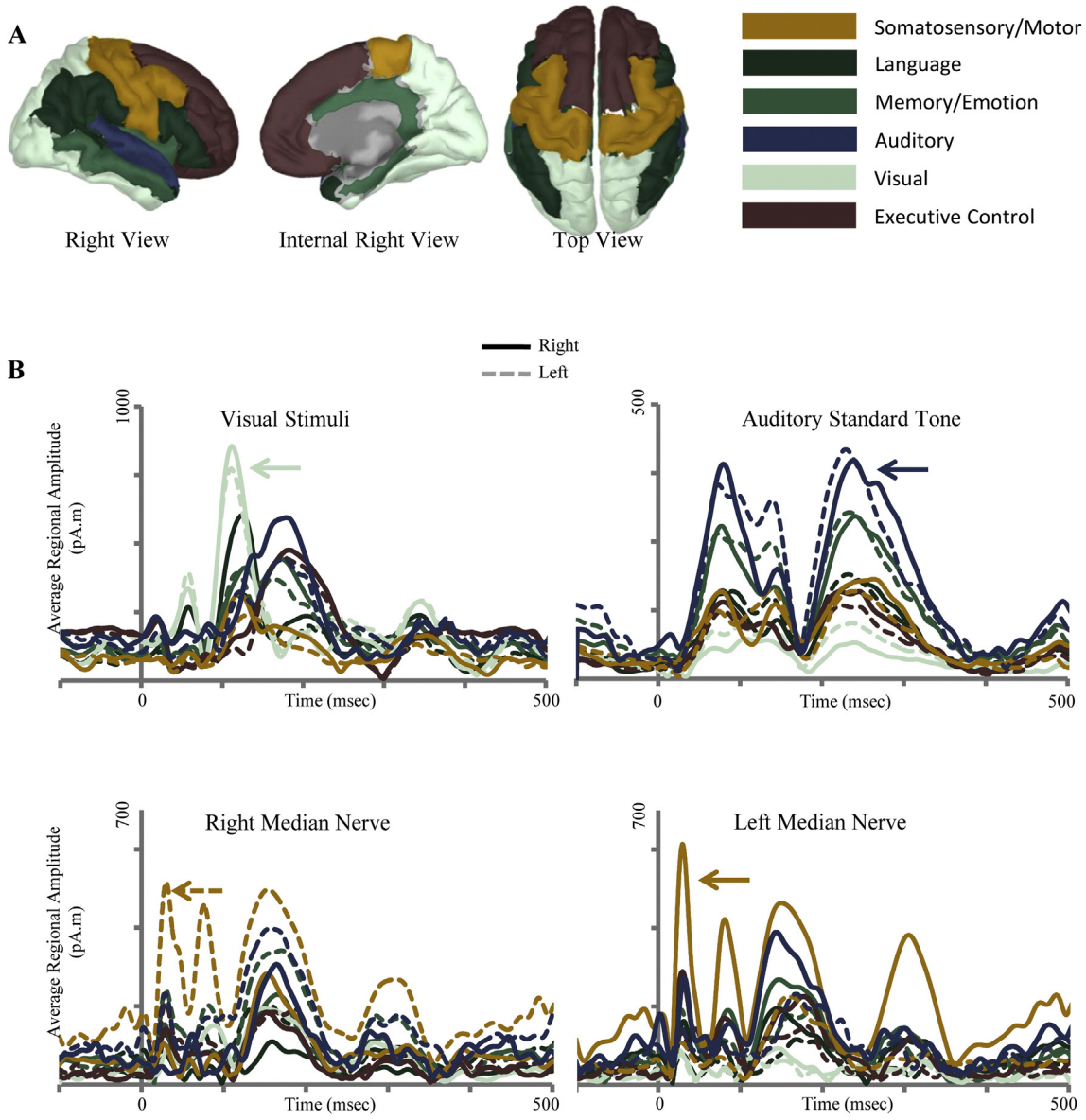

Fig. 4. Cortical region of interest parcellation and activation traces: A: The Desikan-Killiany atlas of 68 cortical regions was parcellated into a coarse-grained cortical division of 12 functional areas, 6 for each hemisphere. B: Average source activation for each cortical region of interest (averaged over all voxels in that region) and for different sensory modalities. Traces filtered at 0.5–40 Hz for visualization. Color coding for different regions corresponds to panel A, with dashed lines representing left sided regions.

consecutive stimuli for each modality (representing a ~2.5 min epoch of stimulation) in all participants. As demonstrated, all values, except two, are positive. These values represent strong preferential activation in the respective cortical area, as expected, both for healthy participants and critically-ill children. These data are also presented in Table 2. Note that for Subject 1 visual and somatosensory data are missing, as detailed in the methods section. Activations for brain areas with anatomically well-defined lesions are indicated by a symbol (*) and in bold font. Of note, even though the responses in brain-injured children were selective to the expected target cortical region, on average the fold activation in these regions was slightly lower than compared to healthy controls. As this was not correlated to anatomically well-defined lesions, we speculate that it reflects non-specific damage to cortical function.

In our sample of brain-injured patients, we identified a total of four brain regions with anatomically well-defined lesions on MRI (and an additional corresponding motor weakness for the somatosensory lesioned regions). We hypothesized that the fold activation in these areas would be lower than the fold activation for respective non-injured areas (in healthy participants and critically-ill children), even though the specificity of the target region activation might still be retained. Indeed, as depicted in Fig. 5B (square markers) and in Table 2, the fold activation in these regions was generally lower ($p < 0.05$, somatosensory response) than the activation for the respective non-injured regions both in healthy and brain-injured patients. For the visual evoked responses we can see that for Subject 5 no preferential activation of the right visual cortex to light flashes was observed even though no occipital anatomical lesion was identified for this patient.

B: Fold activation for different modalities. For each subject and sensory modality depicted (visual, somatosensory and auditory-Standard Tone), the fold activation in the corresponding target functional cortical region was measured relative to activation in a control region at same time-ROI and averaged over 300 consecutive stimulus presentations. Data presented as the logarithm of the fold activation with values above zero representing preferable activation of the target cortical region. Data from right and left hemispheres presented here for all participants. See also Table 2.

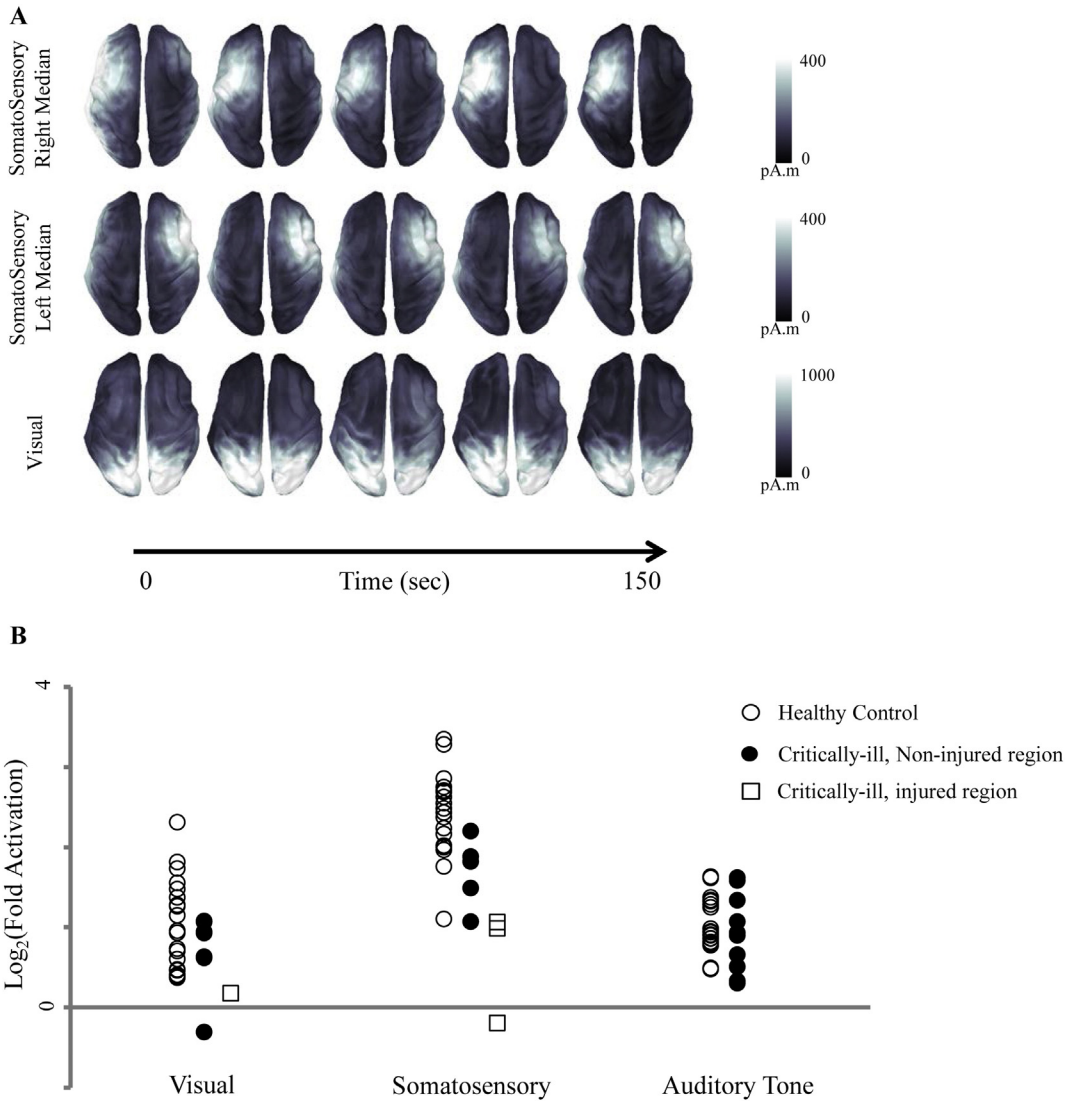

Fig. 5. Towards neuromonitoring using EEG source imaging. A: Repeated cortical source activation estimates for one representative healthy subject. Each row represents five estimates, each derived from the EP trace averaged over 60 consecutive stimulus presentations. The source activation trace was averaged over a time-ROI of either 15–35 msec for the somatosensory stimulation or 50–150 msec for the visual evoked potentials. Somatosensory source estimates were derived from a band-passed EP trace at 30–300 Hz.

Table 1
Subjects description.

#	Age (years) Handedness	Type of brain injury and coma level	Sedative exposure in preceding 24 h
S1	2.5 Not assigned	Severe traumatic brain injury Glasgow Coma Scale score < 8 Intubated and ventilated	Dexmedetomidine 4.25 microgram/kg Fentanyl 2 microgram/kg Lorazepam 0.33 mg/kg Morphine 0.96 mg/kg
S2	6.5 Right	Severe traumatic brain injury Glasgow Coma Scale score < 8 Intubated and ventilated	Diazepam 0.44 mg/kg Lorazepam 0.07 mg/kg Morphine 0.65 mg/kg
S3	16 Right	Hemorrhagic stroke Not intubated	None
S4	13.5 Right	Stroke and cerebral vein thrombosis Not intubated	None
S5	8.5 Right	Acute necrotizing encephalitis Glasgow Coma Scale score < 8 Intubated and ventilated	None

3.4. Proof of concept testing in critically-ill, brain-injured patients

The ability of this system to serve as a bedside functional imaging tool was specifically tested in the intensive care setting in five patients with acute brain injury due to various causes. Three of the patients were unconscious at the time of recording based on Glasgow Coma Scale (GCS) scores <8, and showed a baseline EEG with large amplitude slow wave activity in the Delta range. Brain injury type and pharmacologic exposure to sedatives are detailed in Table 1. Specific source activations for all sensory modalities were elicited for the critically-ill children in the same cortical-ROIs as seen for the healthy participants (Fig. 5B and Table 2. See also example of traces in Fig. 7) albeit less strongly as detailed in the previous subsection.

Fig. 6 demonstrates cortical activation in two of the critically-ill children, specifically examining activation in brain regions that were identified with well-defined injuries by structural MRI or CT scans. Note that in order to preserve right-left consistency the MRI images were flipped horizontally. Panels A and B show the response to somatosensory stimulation of the right and left median nerves for two participants. On MRI and CT, the patient depicted in panel A had evidence of diffuse axonal injury and temporo-parietal injury of the left cortical regions with an associated right-sided weakness on physical exam. This patient exhibited a corresponding reduction of cortical evoked responses in the left somatosensory cortex to right median nerve stimulation. It should be noted that the association between affected regions and the functional cortical activation was not a simple one-to-one correspondence. The same patient exhibited marked and specific activation to auditory stimuli in the left temporal areas with a normal mismatch negativity response despite the anatomical temporal injury. This patient regained full consciousness but remained hemiparetic for over a month post-injury.

In contrast, the patient depicted in panel B had a right pontine hemorrhagic lesion resulting in left hemiparesis and a corresponding reduction of activation in the right somatosensory cortex following left median nerve stimulation. Particularly noteworthy, is that the region of maximum activation for both patients was slightly anterior than the group average of the other participants (compare to Fig. 2). Panel C depicts the same patient as panel B with an additional left occipital hemorrhage and a corresponding reduction in cortical activation localized to the left visual cortex. Fig. 6D, left subpanel, displays cortical activation as projected on the subject's own MRI image while the right subpanel images show the source model solution using a forward model based on the subject's own brain MRI and projecting again to the cortical surface as derived from this MRI. It can be seen that qualitatively, even though there are slight differences in cortical shape and activation profiles, these patterns are similar.

C: same participant as in B. Left subpanel — Horizontally flipped MRI showing left occipital hemorrhage. Right subpanels show average cortical activation over time periods of interest D: Same participant as in B–C. Left subpanel shows cortical activation as projected onto the participant's MRI and right subpanels show the cortical activation as projected and calculated using a head model derived from the participant's MRI.

We quantitatively compared the difference between source activation profiles at the cortical-ROI level as generated using the standard generic MRI to the activation profiles generated using the individual participant's MRI when one was available. Fig. 7A shows an example of the sample activation traces obtained from one patient (S4) in response to Auditory and Somatosensory stimuli. This demonstrates that the activation traces obtained using a template MRI is similar to those obtained using the patient's own MRI. We calculated the correlation coefficients between the average traces generated by using the generic MRI and each patient's MRI, as a basis for head model calculation and source projection, for all patients at each cortical-ROI for all stimuli. The mean correlation was 0.96 ± 0.069. Panel B shows a Bland-Altman plot comparing the normalized source activation. The results indicated good agreement between the source activation obtained using a template MRI and a patient's own MRI scan.

Table 2
Logarithm of Fold activation for each modality: Visual, Somatosentory and Auditory. Activations for brain areas with anatomically well-defined lesions are indicated by a symbol (*) and in bold font.

	Visual		Somatosensory		Auditory		
	Right	Left	Right	Left	Right	Left	
C1	1.15	1.48	2.63	2.71	0.49	1.34	Healthy controls
C2	1.56	1.26	2.86	3.29	1.38	1.29	
C3	0.48	0.71	2.69	2.00	0.94	1.64	
C4	1.38	2.31	2.71	1.76	0.79	0.86	
C5	0.47	0.39	2.43	2.38	0.90	0.81	
C6	0.60	1.74	3.35	2.55	0.78	1.25	
C7	0.96	1.28	2.17	1.97	1.62	0.82	
C8	0.93	1.82	2.24	1.11	0.91	0.86	
C9	0.37	0.74	2.02	2.49	1.33	0.95	
C10	0.41	0.38	2.75	3.28	0.48	0.98	
S1					1.07	0.31	Critically-ill
S2	0.95	1.08	1.07	**0.99***	1.62	0.66	
S3	0.63	**0.18***	**1.07***	1.49	1.34	1.59	
S4	0.62	0.93	2.20	1.82	0.51	0.33	
S5	−0.31	1.07	**−0.19***	1.88	0.90	0.93	

4. Discussion

This is a proof of concept study which demonstrates the use of high-density EEG in combination with multi-modal sensory stimulation and source modelling to generate functional brain activation maps in critically-ill patients with acute brain injuries. We provided the first demonstration of selective, source level monitoring of functional brain responses to multiple sensory modalities in children with acute brain injuries in the intensive care setting. Reduced activation in specific brain systems appears to correspond to the location of injury, and does not require the participant's individual brain MRI for system-specific monitoring of functional brain responses.

This set-up was also designed to examine higher-level cortical processing by using an oddball auditory paradigm involving the subject's own name. Interestingly, while all healthy controls and brain-injured children showed a markedly larger response to their own name compared to the standard vowel-changed name, it was not significantly larger, on average, than the response to the other deviant name. This is likely influenced by our choice to focus on a relatively large cortical-ROI within this study.

A limitation of our study lies in our choice not to perform multiple runs of each stimulation paradigm to evaluate reproducibility. As for each participant and stimulation modality we have hundreds of repetitions, we ensured that within each “run” the responses were consistent as can be seen for example in Fig. 5A and elaborated in the methods section. However, we plan in the future a more thorough clinical validation of this set-up and this subject will be then addressed. We have also not performed formal auditory evaluation of our participants prior to recording acknowledging that peripheral attenuation might skew the cortical activation. As stimuli were presented binaurally through headphones, and there is bi-laterality to auditory cortices (60% contralateral, 40% ipsilateral) these effects are probably not major.

The major limitation of this study lies in the relatively small number of children with acute brain injury included in the analysis. Such a small sample size did not allow us to extensively validate normal and pathologic activation ranges or to fully characterize the association between functional images created by this system and anatomic injury. For example, there is a well described variability of the waveform pattern, amplitude, and scalp topography of flash evoked visual responses and asymmetric responses have been reported even in normal subjects with normal functional vision. In our study for example, subject 5

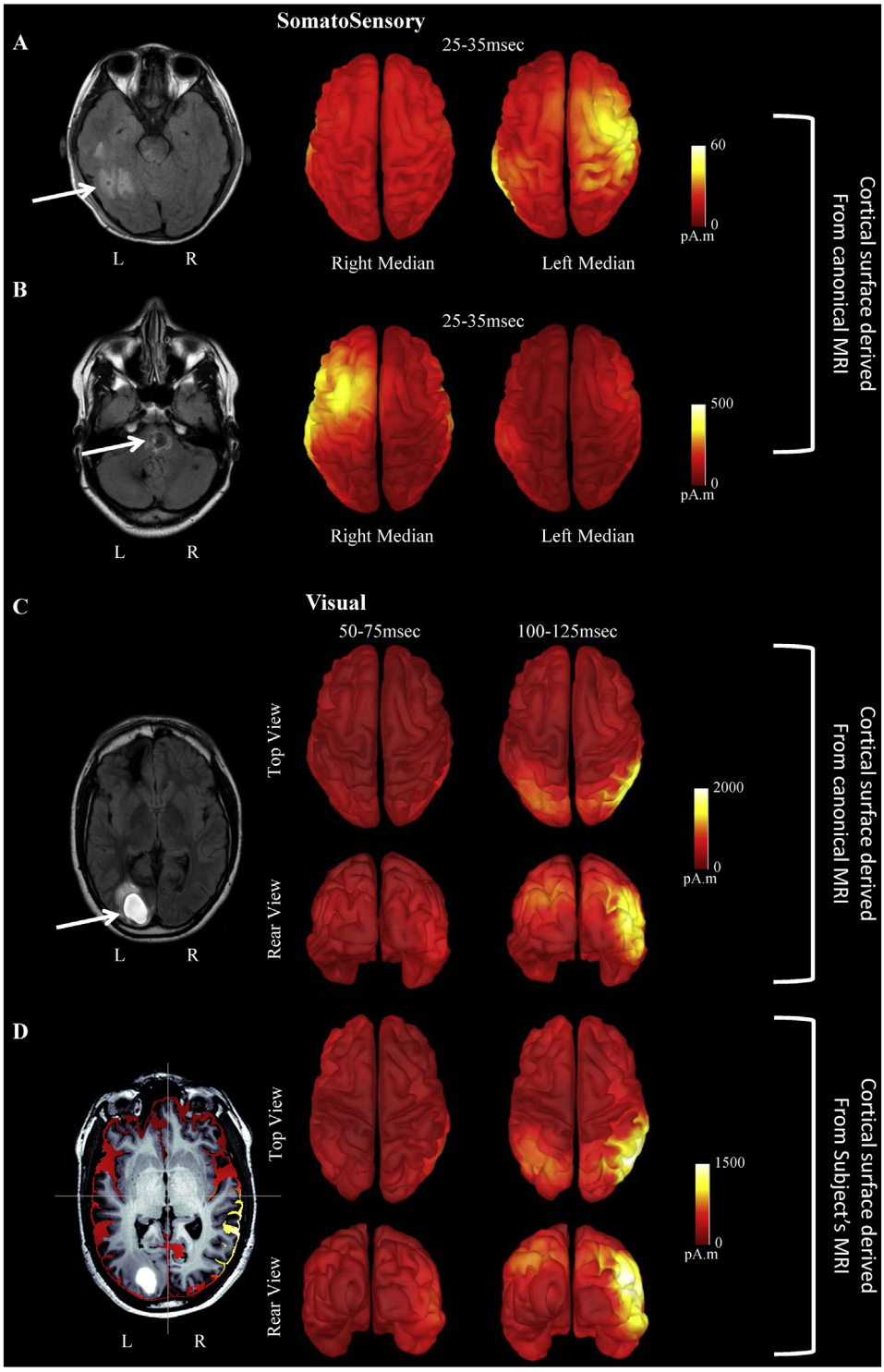

Fig. 6. Cortical activation in brain-injured participants: A + B: for two different participants: left subpanels — horizontally flipped MRI axial FLAIR image depicting left temporal-occipital and right Pontine injury respectively and marked by arrows. Right subpanels — cortical activation to somatosensory stimulation at 25–35 msec post-stimulus, projected from the average band-passed EP trace at 30–300 Hz.

demonstrated a low activation of the right occipital region to light flashes (Table 2) even though no corresponding anatomical injury was identified. This might be due to the inherent variability of the evoked response, a difference between functional and anatomical injury or even due to the fact that this specific subject had a thalamic injury that might have affected the cortical responses. Thus, future studies with a larger sample size are planned to address this limitation and quantify in depth the relative contributions of the "normal" variation versus brain injury effects.

Moreover, as this set-up relies on EEG source imaging to generate cortical activation maps, it suffers from the known limitations of these approaches (Michel et al. 2004; Michel and Murray 2012). Specifically, in the context of brain injuries there might be conductivity changes that affect the forward model (Irimia et al. 2013a; Irimia et al. 2013b)

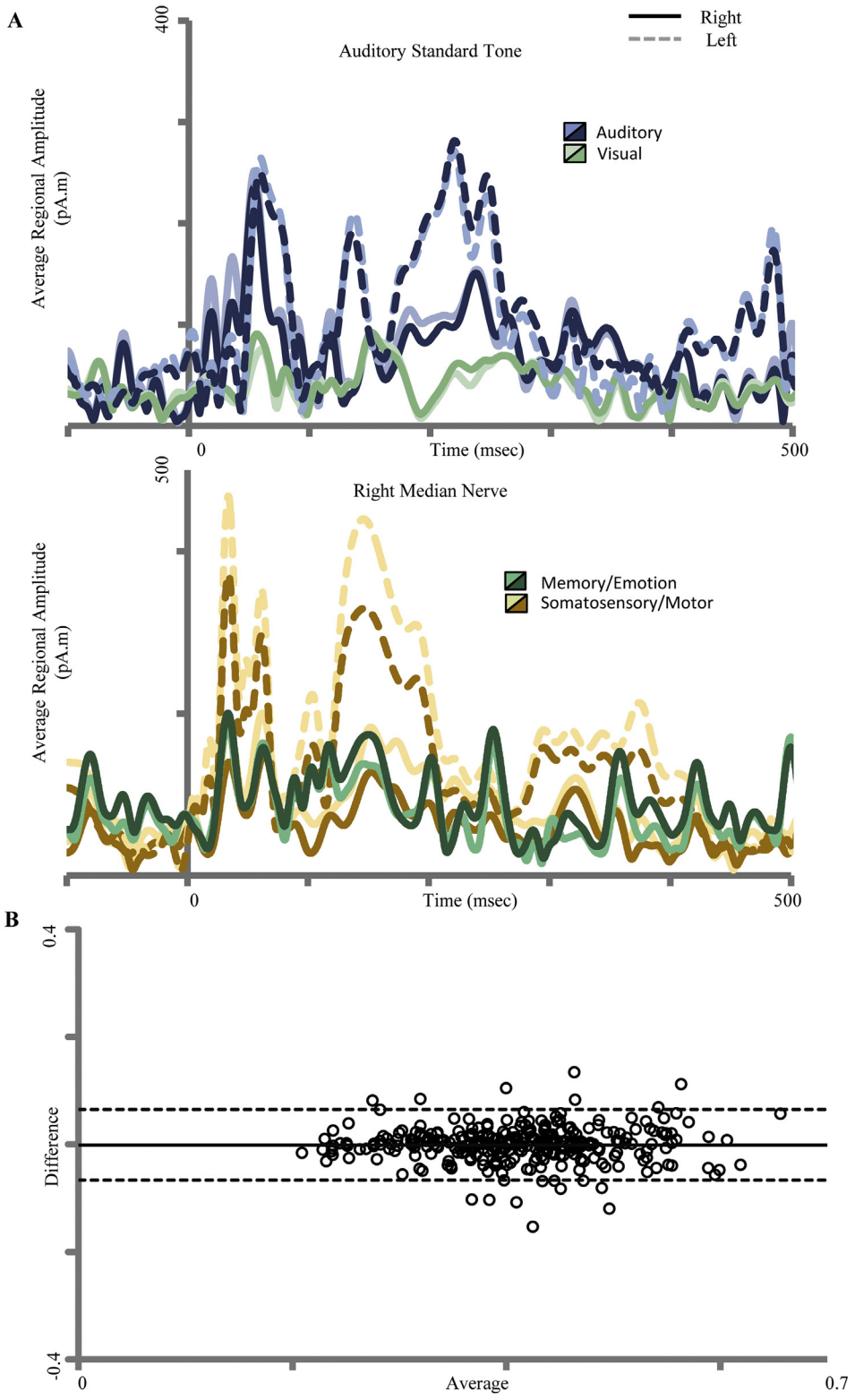

Fig. 7. Impact of template compared to participant's MRI for head modeling and source projection. A: Sample average cortical activation traces obtained from one participant in response to standard auditory tone and somatosensory stimuli. The darker traces correspond to the activation profile generated using the patient's own MRI, while the lighter traces correspond to the activation profile using the generic MRI. Traces were filtered at 0.5–40 Hz for visualization. B: Bland-Altman plot comparing the average normalized source activations as obtained using either MRI for all patients. Dashed lines represent ±2SD.

and localization accuracy. In addition, our study used a generic head model and when possible compared to the sources generated by the participant's MRI, without a marked difference in results. This is probably due to other generators of spatial localization inaccuracies that have a larger effect and our choice of relatively large cortical-ROIs to average activations across. Since this tool intended to be used to examine changes in cortical activity at a relatively low spatial resolution, the importance of these is probably secondary. This is advantageous as it indicates that monitoring activation in various functional systems using EEG is feasible even when a patients MRI is not available. Future

research using a larger number of patients recorded with this set-up may enable imaging with a better spatial resolution, a better algorithmic/automated choice of time and cortical regions of interest and perhaps a characterization of the association with outcome and anatomical injury.

We would like to emphasize that the quality and integrity of the signals is of paramount importance to ensure at every step, in order to avoid errors before moving to the segmentation phases of the analyses, and before using this approach to make individual clinical decisions.

In summary, if employed in a continuous fashion, we forecast that a portable bedside functional imaging system, as described above, could be used for diagnosis and real-time early detection of secondary deteriorations that may manifest as changes in activation patterns at the cortical-ROI level and judiciously for prognostication. Moreover, in the future such a system may be used to guide treatment according to functional individual responses rather than arbitrary thresholds.

Currently, source localization methods and software used for off-line analysis in this study are applied for research and not for clinical care related decisions. The present study illustrates an initial proof of concept for the feasibility of such a system for obtaining functional responses from particular brain systems in an intensive care setting. Further research is needed prior to considering this a clinical tool.

Financial support

Department of Critical Care Research Fund. Canadian Foundation for Innovation (CFI) for the Centre for the Investigation of Neuroplasticity and Developmental Disorders 2006–2011. Project #11954.

Acknowledgments

The authors are grateful to Roy Sharma and Eric Niles for providing invaluable technical assistance and support in setting up the experiment logistics and to Dr. Cecil Hahn for discussions in the early stages of this study.

References

Moreau, J.F., Fink, E.L., Hartman, M.E., Angus, D.C., Bell, M.J., Linde-Zwirble, W.T., Watson, R.S., 2013. Hospitalizations of children with neurologic disorders in the United States. Pediatr. Crit. Care Med. 14, 801–810.

Parslow, R.C., Morris, K.P., Tasker, R.C., Forsyth, R.J., Hawley, C.A., 2005. Epidemiology of traumatic brain injury in children receiving intensive care in the UK. Arch. Dis. Child. 90, 1182–1187.

Geocadin, R.G., Koenig, M.A., Jia, X., Stevens, R.D., Peberdy, M.A., 2008. Management of brain injury after resuscitation from cardiac arrest. Neurol. Clin. 26, 487–506 (ix).

Corso, P., Finkelstein, E., Miller, T., Fiebelkorn, I., Zaloshnja, E., 2006. Incidence and lifetime costs of injuries in the United States. Inj. Prev. 12, 212–218.

Perkins, E., Stephens, J., Xiang, H., Lo, W., 2009. The cost of pediatric stroke acute care in the United States. Stroke 40, 2820–2827.

Vidgeon, S.D., Strong, A.J., 2011. Multimodal cerebral monitoring in traumatic brain injury. J. Intensive Care Soc. 12, 126–133.

Niedermeyer, E., da Silva, F.L., 2005. Electroencephalography: Basic Principles, Clinical Applications, and Related Fields. Lippincott Williams & Wilkins.

Buzsáki, G., Traub, R.D., Pedley, T., 2003. The cellular synaptic generation of EEG activity. In: Ebersole, J.S., Pedley, T.A. (Eds.), Current Practice of Clinical Encephalography, pp. 1–11.

Ebersole, J.S., 2003. Cortical Generators and EEG Voltage Fields. Lippincott Williams & Wilkins, Philadelphia, pp. 12–31.

Singh, M., Kim, S., Kim, T.S., 2003. Correlation between BOLD-fMRI and EEG signal changes in response to visual stimulus frequency in humans. Magn. Reson. Med. 49, 108–114.

Duncan, C.C., Summers, A.C., Perla, E.J., Coburn, K.L., Mirsky, A.F., 2011. Evaluation of traumatic brain injury: brain potentials in diagnosis, function, and prognosis. Int. J. Psychophysiol. 82, 24–40.

Nenadovic, V., Hutchison, J.S., Dominguez, L.G., Otsubo, H., Gray, M.P., Sharma, R., Belkas, J., Velazquez, J.L.P., 2008. Fluctuations in cortical synchronization in pediatric traumatic brain injury. J. Neurotrauma 25, 615–627.

Ramachandran Nair, R., Sharma, R., Weiss, S.K., Cortez, M.A., 2005. Reactive EEG patterns in pediatric coma. Pediatr. Neurol. 33, 345–349.

Wijdicks, E.F., Hijdra, A., Young, G., Bassetti, C., Wiebe, S., 2006. Practice parameter: prediction of outcome in comatose survivors after cardiopulmonary resuscitation (an evidence-based review) report of the quality standards Subcommittee of the American Academy of Neurology. Neurology 67, 203–210.

Nishisaki, A., Sullivan 3rd, J., Steger, B., Bayer, C.R., Dlugos, D., Lin, R., Ichord, R., Helfaer, M.A., Nadkarni, V., 2007. Retrospective analysis of the prognostic value of electroencephalography patterns obtained in pediatric in-hospital cardiac arrest survivors during three years. Pediatr. Crit. Care Med. 8, 10–17.

Lehembre, R., Gosseries, O., Lugo, Z., Jedidi, Z., Chatelle, C., Sadzot, B., Laureys, S., Noirhomme, Q., 2012. Electrophysiological investigations of brain function in coma, vegetative and minimally conscious patients. Arch. Ital. Biol. 150, 122–139.

Picton, T., Bentin, S., Berg, P., Donchin, E., Hillyard, S., Johnson, R., Miller, G., Ritter, W., Ruchkin, D., Rugg, M., 2000. Guidelines for using human event-related potentials to study cognition: recording standards and publication criteria. Psychophysiology 37, 127–152.

Fernandez-Espejo, D., Owen, A.M., 2013. Detecting awareness after severe brain injury. Nat. Rev. Neurosci. 14, 801–809.

Fischer, C., Dailler, F., Morlet, D., 2008. Novelty P3 elicited by the subject's own name in comatose patients. Clin. Neurophysiol. 119, 2224–2230.

Daltrozzo, J., Wioland, N., Mutschler, V., Kotchoubey, B., 2007. Predicting coma and other low responsive patients outcome using event-related brain potentials: a meta-analysis. Clin. Neurophysiol. 118, 606–614.

Robinson, L.R., Micklesen, P.J., Tirschwell, D.L., Lew, H.L., 2003. Predictive value of somatosensory evoked potentials for awakening from coma*. Crit. Care Med. 31, 960–967.

Folmer, R.L., Billings, C.J., Diedesch-Rouse, A.C., Gallun, F.J., Lew, H.L., 2011. Electrophysiological assessments of cognition and sensory processing in TBI: applications for diagnosis, prognosis and rehabilitation. Int. J. Psychophysiol. 82, 4–15.

Lew, H.L., Poole, J.H., Castaneda, A., Salerno, R.M., Gray, M., 2006. Prognostic value of evoked and event-related potentials in moderate to severe brain injury. J. Head Trauma Rehabil. 21, 350–360.

Kane, N.M., Curry, S.H., Rowlands, C.A., Manara, A.R., Lewis, T., Moss, T., Cummins, B.H., Butler, S.R., 1996. Event-related potentials–neurophysiological tools for predicting emergence and early outcome from traumatic coma. Intensive Care Med. 22, 39–46.

Amantini, A., Fossi, S., Grippo, A., Innocenti, P., Amadori, A., Bucciardini, L., Cossu, C., Nardini, C., Scarpelli, S., Roma, V., 2009. Continuous EEG-SEP monitoring in severe brain injury. Neurophysiol. Clin. 39, 85–93.

Lee, A.K., Larson, E., Maddox, R.K., Shinn-Cunningham, B.G., 2014. Using neuroimaging to understand the cortical mechanisms of auditory selective attention. Hear. Res. 307, 111–120.

Murray, M.M., Michel, C.M., Grave de Peralta, R., Ortigue, S., Brunet, D., Gonzalez Andino, S., Schnider, A., 2004. Rapid discrimination of visual and multisensory memories revealed by electrical neuroimaging. NeuroImage 21, 125–135.

Harrison, A.H., Connolly, J.F., 2013. Finding a way in: a review and practical evaluation of fMRI and EEG for detection and assessment in disorders of consciousness. Neurosci. Biobehav. Rev. 37, 1403–1419.

Irimia, A., Goh, S.Y., Torgerson, C.M., Chambers, M.C., Kikinis, R., Van Horn, J.D., 2013a. Forward and inverse electroencephalographic modeling in health and in acute traumatic brain injury. Clin. Neurophysiol. 124, 2129–2145.

Irimia, A., Goh, S.Y., Torgerson, C.M., Stein, N.R., Chambers, M.C., Vespa, P.M., Van Horn, J.D., 2013b. Electroencephalographic inverse localization of brain activity in acute traumatic brain injury as a guide to surgery, monitoring and treatment. Clin. Neurol. Neurosurg. 115, 2159–2165.

Guideline 5, 2006. Guidelines for standard electrode position nomenclature. Clin. Neurophysiol. 23, 107–110.

Cuffin, B.N., 2001. Effects of modeling errors and EEG measurement montage on source localization accuracy. Clin. Neurophysiol. 18, 37–44.

Michel, C.M., Murray, M.M., Lantz, G., Gonzalez, S., Spinelli, L., Grave de Peralta, R., 2004. EEG source imaging. Clin. Neurophysiol. 115, 2195–2222.

Brainard, D.H., 1997. The psychophysics toolbox. Spat. Vis. 10, 433–436.

Staffen, W., Kronbichler, M., Aichhorn, M., Mair, A., Ladurner, G., 2006. Selective brain activity in response to one's own name in the persistent vegetative state. J. Neurol. Neurosurg. Psychiatry 77, 1383–1384.

Berlad, I., Pratt, H., 1995. P300 in response to the subject's own name. Electroencephalogr. Clin. Neurophysiol. 96, 472–474.

Schiff, N.D., Nauvel, T., Victor, J.D., 2014. Large-scale brain dynamics in disorders of consciousness. Curr. Opin. Neurobiol. 25, 7–14.

Hirsch, L.J., 2004. Continuous EEG monitoring in the intensive care unit: an overview. J. Clin. Neurophysiol. 21, 332–340.

Michel, C.M., Murray, M.M., 2012. Towards the utilization of EEG as a brain imaging tool. NeuroImage 61, 371–385.

Brodbeck, V., Spinelli, L., Lascano, A.M., Wissmeier, M., Vargas, M.I., Vulliemoz, S., Pollo, C., Schaller, K., Michel, C.M., Seeck, M., 2011. Electroencephalographic source imaging: a prospective study of 152 operated epileptic patients. Brain J. Neurol. 134, 2887–2897.

Tadel, F., Baillet, S., Mosher, J.C., Pantazis, D., Leahy, R.M., 2011. Brainstorm: a user-friendly application for MEG/EEG analysis. Comput. Intell. Neurosci. 2011, 879716.

Berg, P., Scherg, M., 1994. A fast method for forward computation of multiple-shell spherical head models. Electroencephalogr. Clin. Neurophysiol. 90, 58–64.

Holmes, C.J., Hoge, R., Collins, L., Woods, R., Toga, A.W., Evans, A.C., 1998. Enhancement of MR images using registration for signal averaging. J. Comput. Assist. Tomogr. 22, 324–333.

Shattuck, D.W., Leahy, R.M., 2002. BrainSuite: an automated cortical surface identification tool. Med. Image Anal. 6, 129–142.

Pascual-Marqui, R.D., Michel, C.M., Lehmann, D., 1994. Low resolution electromagnetic tomography: a new method for localizing electrical activity in the brain. Int. J. Psychophysiol. 18, 49–65.

Pascual-Marqui, R.D., 2002. Standardized low-resolution brain electromagnetic tomography (sLORETA): technical details. Methods Find. Exp. Clin. Pharmacol. 24, 5–12 (Suppl D).

Evans, A.C., Collins, D.L., Mills, S., Brown, E., Kelly, R., Peters, T.M., 1993. 3D statistical neuroanatomical models from 305 MRI volumes. Nuclear Science Symposium and Medical Imaging Conference, 1993, 1993 IEEE Conference Record: IEEE, pp. 1813–1817.

Desikan, R.S., Segonne, F., Fischl, B., Quinn, B.T., Dickerson, B.C., Blacker, D., Buckner, R.L., Dale, A.M., Maguire, R.P., Hyman, B.T., Albert, M.S., Killiany, R.J., 2006. An automated labeling system for subdividing the human cerebral cortex on MRI scans into gyral based regions of interest. NeuroImage 31, 968–980.

Mento, G., Tarantino, V., Sarlo, M., Bisiacchi, P.S., 2013. Automatic temporal expectancy: a high-density event-related potential study. PLoS One 8.

Di Russo, F., Martinez, A., Sereno, M.I., Pitzalis, S., Hillyard, S.A., 2002. Cortical sources of the early components of the visual evoked potential. Hum. Brain Mapp. 15, 95–111.